Available online at www.sciencedirect.com
ScienceDirect
Trans. Nonferrous Met. Soc. China 21(2011) s536−s542
Transactions of Nonferrous Metals Society of China
www.tnmsc.cn

Extending dynamic models of mining subsidence

LIAN Xu-gang[1, 2], Andrew JAROSZ[2], Jose SAAVEDRA-ROSAS[2], DAI Hua-yang[1]
1. College of Geoscience and Surveying Engineering, China University of Mining and Technology, Beijing 100083, China;
2. Western Australian School of Mines, Curtin University, Kalgoorlie 6430, Australia

Received 19 June 2011; accepted 10 November 2011

Abstract: The movement and deformation processes of the overburden strata and ground surface, induced by underground mining, are affected by mining method, spatial relationships, geotechnical conditions of the rock strata and time. The authors reviewed and extended an existing classical prediction model of the dynamic subsidence, and proposed potential new research avenues offered by Cellular Automata (CA) models. The Knothe's influence function model and the significance of subcritical mining geometry were analyzed. The prediction results were verified against the subsidence field survey data to assess their quality and acceptability.
Key words: dynamic subsidence; subsidence prediction; cellular automata

1 Introduction

The movements and deformations of the overburden strata and ground surface, due to the underground mining, are complex processes affected by the mining method and geometry, spatial relationship between deformation instance and mining panels, timing of the extraction process, composition and geotechnical parameters of the overburden and the dynamics of deformation processes transferred to the ground surface. Up to date, the following solutions focusing on the prediction of mining induced subsidence has been analysed and proposed: 1) Time function models based on the Mitscherlich's "law of growth" adopted by KNOTHE [1] and applied by JAROSZ et al [2], CHANG et al [3] and CUI et al [4]; 2) Models utilising the rheological characteristics of overburden strata to derive surface subsidence over time applied by DJAMALUDDIN et al [5]; 3) Empirical models based on the measurements of surface deformations presented by YU et al [6], ZENG et al [7] and DENG et al [8]; 4) Numerical simulation models adopted by ADAMEK et al [9], FALON et al [10], YANG et al [11] and LI et al [12].

The basic mechanism inducing subsidence is linked to the advance of a working face, which modifies the size of the extraction panel (void) and to the subsequent transference of this instability throughout the overburden to the surface. For illustration purposes, the model initially proposed by KNOTHE [1] is reviewed in more details in the following section of this paper. However, the objective is not to reproduce in details the previously proposed solutions, but rather to expand the model's applicability particularly to the subcritical extraction cases. This exercise should also be instrumental in establishing a state of the art platform for possible future studies. The potential implementation of a Cellular Automata (CA) model is also discussed later in this work. The theoretical analysis suggests that the application of the CA model should lead to the results that are coherent with the classical influence function and the stochastic models that are well established in the subsidence prediction practice. Taking into account the advances in the computational techniques and computational capabilities of the current computer hardware, the proposed CA approach could lead to the development of new efficient subsidence calculation methods.

2 Knothe's model of dynamic subsidence

The Mitscherlich's law of the growth applied to the case of dynamic subsidence involves consideration of the subsidence rate $\mathrm{d}W(t)/\mathrm{d}t$, the final (asymptotic) value of subsidence $W^f(t)$ and the current value of subsidence

Foundation item: Project (200911036) supported by the Ministry of Land and Resources Research Special; Project (50974122) supported by the National Natural Science Foundation of China; Project (2010YD05) supported by the Fundamental Research Funds for the Central Universities
Corresponding author: Andrew JAROSZ; E-mail: a.jarosz@curtin.edu.au

$W(t)$ at the time t. The mathematical expression used by Knothe [1] has the following form:

$$\frac{\mathrm{d}W(t)}{\mathrm{d}t}=c[W^f(t)-W(t)] \tag{1}$$

where c is termed as the time coefficient, which defines the impacts of geological and mining conditions on the rate of deformation process. By introducing, originally proposed by Knothe, the subsidence influence function based on the Gaussian (normal) probability distribution:

$$W^f(x_0,x_t,S)=\frac{W_{\max}}{r^2}\iint_S \exp(-\pi\frac{x^2+y^2}{r^2})\mathrm{d}S \tag{2}$$

where $W_{\max}$ is maximum subsidence, $W_{\max}=qm\cos\alpha$; q is subsidence factor; m is extraction thickness; α is dip angle of a coal seam; r is the radius of influence; S is extraction area.

The following closed form solution can be obtained for a panel with one mining face moving toward the point (Fig. 1) where subsidence is to be defined [2]:

$$\begin{aligned}W(x_0,x_t,\Delta t)=W^f(x_0,x_t)-\exp(\frac{u^2}{4\pi}+\frac{u}{r}x_t)\cdot\\ W^f(x_0+\frac{ur}{2\pi},x_t+\frac{ur}{2\pi})+\Delta W^f(x_0,x_t)\cdot\\ [1-\exp(-c\Delta t)]\end{aligned} \tag{3}$$

where $W^f(x_0, x_t)$ is the final subsidence at stop time t; v is rate of advance of a mining face; $u=-cr/v$; c is time coefficient; Δt is time after a mining face stopped (for advancing face, Δt=0).

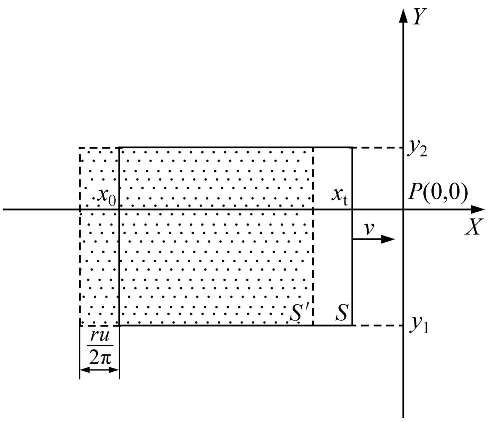

Fig. 1 Geometry of longwall panel with advancing face and translated extraction contour

The above solution introduces three stages of the subsidence development over time.

1) Subsidence development while the face is advancing with constant speed v (Δt=0), which is represented by the first two terms.

2) Subsidence development after the face has stopped (Δt>0) and until local maximum subsidence is reached, which is represented by all three terms.

3) Final (asymptotic) subsidence, which is represented by the first term only.

It can be seen in the Eq. (3) that after the mining face is stopped, the remaining portion of the subsidence can be defined as:

$$\Delta W^f(x_0,x_t)=\exp(\frac{u^2}{4\pi}+\frac{u}{r}x_t)\cdot W^f(x_0+\frac{ur}{2\pi},x_t+\frac{ur}{2\pi}) \tag{4}$$

The above leads to the following solution for the subsidence development phase after the face of the mining panel stopped:

$$\begin{aligned}W(x_0,x_t,\Delta t)=W^f(x_0,x_t)-\\ \exp(\frac{u^2}{4\pi}+\frac{u}{r}x_t-c\Delta t)\cdot W^f(x_0+\frac{ur}{2\pi},x_t+\frac{ur}{2\pi})\end{aligned} \tag{5}$$

3 Impact of sub-critical panel's dimensions

The extraction panels classified as critical or super-critical, in the sense of surface subsidence, are panels with horizontal dimensions, in any direction, equal or greater than $2r$ (2 times radius of influence) or 1.2−1.4 of average mining depth. Such panels will develop the subsidence troughs with at least one point achieving the maximum possible subsidence for the existing geotechnical conditions of overburden. The value of maximum subsidence can be calculated using the following simple empirical formulae:

$$W_{\max}=qm\cos\alpha \tag{6}$$

where q is an empirical subsidence factor, m represents the seam thickness, and α represents the seam dip angle.

In case of the sub-critical panels, with one of the dimensions less than $2r$ (this usually applies to the panel width < $2r$ or panel width ranging in 1.2−1.4 of the average mining depth), the developing subsidence does not achieve the maximum possible subsidence for large extraction areas. The smaller subsidence results not only from a small area of extraction but also from different behaviours of the overburden strata. To adjust these sub-critical conditions, a variable subsidence factor q_s can be introduced to the previously listed Eq. (6). The relation between the sub-critical and critical subsidence factors can be expressed as: $q_s=q\rho k_D$, where ρ is a proportionality function depending on the directional ratio (k_D) between the panel width (in the particular direction) and the average mining depth (H_0), i.e. $k_D=D/H_0$.

The issue of critical dimension should be applied to both, the width and the length of an extraction panel. As a result the subsidence factors can be calculated as follows:

1) For the panels characterised by less than critical width (D<(1.2−1.4)H_0), the initial panel advance will also be subcritical (D_t<(1.2−1.4)H_0) and the subsidence factor will be calculated as:

$$q_s = q\sqrt{\rho(k_{D_t})\rho(k_D)} \tag{7}$$

where D represents the final dimension (s) of a panel, D_t represents dimension (S) at a specific time t of panel development, k_D represents directional ratio.

When the panel advance reaches the critical stage and after it, the subsidence factor will be calculated as $q_s=q\rho(k_D)$.

2) For the panels characterised by critical and super-critical width (D≥(1.2−1.4)H_0), at the initial stage of panel advance (advance less then critical), the subsidence factor will be calculated as: $q_s = q\rho(k_{D_t})$.

After the panel advance reaches the critical dimensions: $q_s=q$.

The analyses of the field case studies, from Huainan mining area in China, suggest that a Boltzmann type function [12] can represent well the variation of subsidence proportionality factor $\rho(k_D)$ in relation to horizontal dimensions of an extraction panel. The basic form of a Boltzmann function is as follows:

$$\rho(k) = A_2 + \frac{A_1 - A_2}{1+\exp[(k-A_3)/A_4]} \tag{8}$$

where $k = k_D$ or k_{D_t}, A_1, A_2, A_3, A_4 are empirical factors defined from field data.

An example of a Boltzmann curve defined for the Huainan mine area in China is presented in Fig. 2.

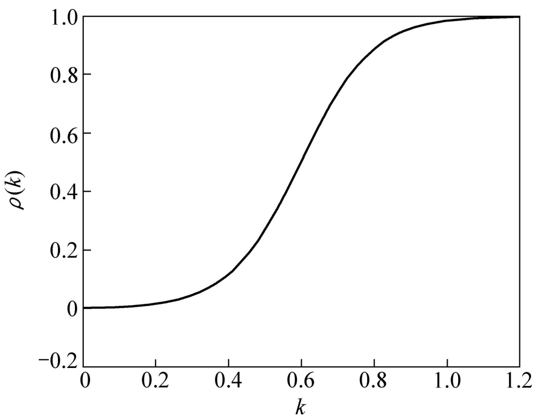

Fig. 2 Boltzmann curve for Huainan mine area in China

For the mining areas, with insufficient field data to define the exact form of a Boltzmann function, the following can be applied:

$$\rho(k_D) = k_1 k_D \tag{9}$$

$$\rho(k_{D_t}) = k_3 k_{D_t} \tag{10}$$

where k_1, k_3 are factors determined according to the geotechnical properties of overburden strata, viz.:

$$k_1, k_3 = \begin{cases} 0.7, \text{ soft stratum} \\ 0.8, \text{ medium stratum} \\ 0.9, \text{ hard stratum} \end{cases} \tag{11}$$

4 Case study

The presented case study is based on the deformation measurements collected above a coalmine panel in the Huainan mining area, Anhui Province, China. The panel geometry was characterised by a length of 620 m and a width of 162 m. The average mining depth was 500 m, which included 100 m of the competent rock strata above the coal seam and 400 m of the loose material above it. The extraction method used was the longwall mechanical mining with caving.

The collected subsidence data was used to determine the basic subsidence prediction parameters including: subsidence factor, edge effect, influence angle, subsidence deviation angle from vertical, horizontal movement proportionality factor, and time coefficient. It has to be noted that the face advance was considered constant, whereas the reality indicated that the advance rates are usually variable. The constant rate was calculated by dividing the total face advance distance by the time required to extract the panel.

The plan view of longwall panel and the position of monitoring (prediction) line on the surface are presented in Fig. 3. The graphical comparison of the measured and predicted subsidence at progressive stages of the panel development can be seen in Fig. 4. The corresponding absolute deviations between predicted and measured subsidence are presented in Fig. 5.

The maximum subsidence deviation in relation to the maximum subsidence is about 12%. This level of deviation could suggest that the proposed subsidence prediction method yields acceptable results, however, the authors believe that much better prediction could be achieved through further refinement of the proposed prediction model. At this stage the model is not capable to account for differences in overburden strata composition. The distribution of deviations, presented in Fig. 5, suggests that the proposed model's quality is poorer at the edges of extraction panel. The authors also believe that this could be originated by the variation in the rock composition of the overburden strata and it should have more pronounced impacts on the development of subsidence in the areas the above edges of extraction panels.

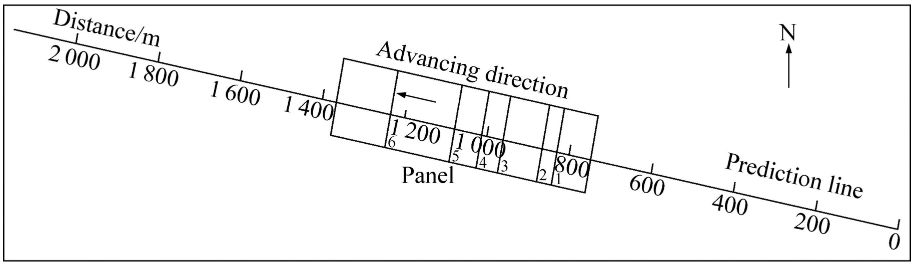

Fig. 3 Plan view of panel and prediction line (1−6 are position line of each mining phase)

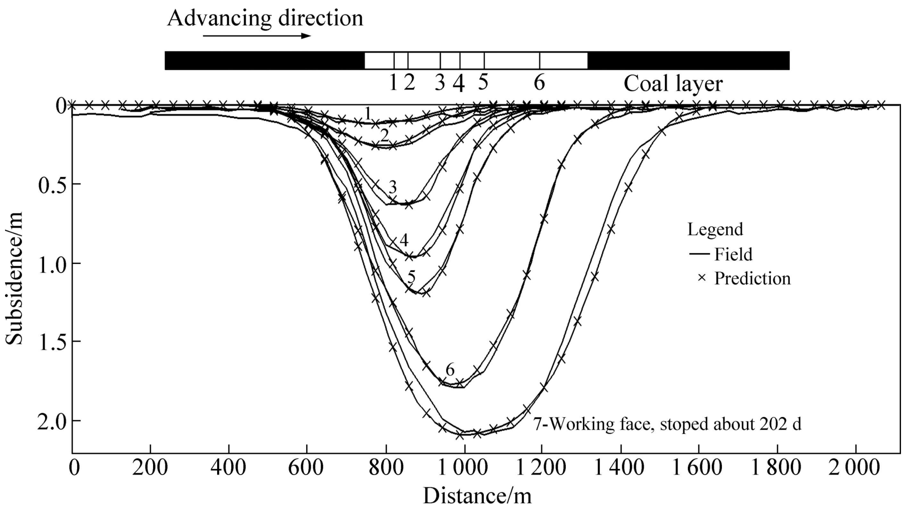

Fig. 4 Comparison between predicted and field subsidence curves

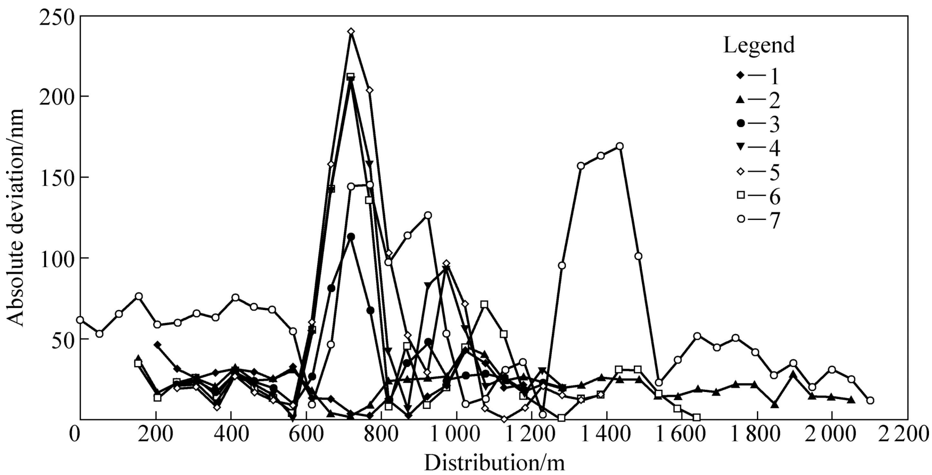

Fig. 5 Absolute deviation between predicted and field subsidence

5 Cellular Automata (CA) models and its potential for subsidence prediction

In Ref. [14] a new cellular automata model was introduced for the specific purposes of modelling gravitational flow. Some authors used CA to model gravitational flow of granular medium (sand) [15−18]. Specific applications to mining the gravitational flow are much less frequent. Attempts have been made to model the gravitational flow phenomena with a view towards mining applications [19−22] by using CA.

The model presented by ALFARO and SAAVEDRA [14] was originally developed to simulate the behaviour of sand models of gravitational flow. A closer look at the results presented in that paper reveals a reasonable similarity between the subsidence theory already discussed in this paper and the results obtainable using a computational model based on CA. The authors believed the computational model presented therein could be used in the context of subsidence prediction and consequently the authors proposed to explore this research avenue in the near future. One of the most attractive features of the CA based model is its apparent flexibility which could be used to extend the current state of the art in the subsidence prediction to the next level by making extensive use of never and more powerful computational capabilities not existent in the past. In order to better understand better what this novel model is about a light introduction to Cellular Automata theory [23] is provided:

A cellular automaton is an array of cells each colored either black or white. At every step there is a definite rule that determines the color of a given cell from the color of that cell and its neighbors on the step before.

The main characteristics of a cellular automaton are as follows: 1) Its state, which is variable for each cell; 2) Its neighbourhood, the set of cells, which interacts with the cell in question; 3) The set of rules or program: gives the changes in state with respect the neighbours.

The CA proposed in Ref. [14] uses as cubed cell pattern. For this CA cells can be used in two possible states: full or empty. At the beginning all cells are full. When a cell is extracted, the generated void must be filled with material from another cell; the cells above the current void are in privileged position to accomplish this objective. Inspired by this idea a transition rule for the evolution of the CA was proposed. A probability distribution for the neighbours (the upper cells) is assigned, and then a selection is performed according to this distribution for the cell, which replaces the void. The void now has been moved to the position of the previously selected cell. This process is repeated until the void reaches the surface (the last level of cells). For illustration purposes an example of a neighbourhood in two dimensions is presented.

After this first void reaches the surface, a new void is generated by the extraction of a new cell from the same position used before which represents draw-points in block caving but can be extended to more general settings. The ascending void generated by the extraction of a cell was named by ALFARO and SAAVEDRA [14] as a “bubble”.

CALDERON et al [24] presented an algorithm to calibrate the transition probabilities. They based their algorithm in the diameter of the opening at a certain height. This approach was proven to be effective but in practical terms depended on the information that was not known as priori and was believed to be difficult to obtain. The interesting fact is that an algorithm is available that can be used to calibrate the transition probabilities and it is envisioned that it could easily be adapted in the context of subsidence applications where usually data is available.

5.1 Bubbling process

The proposed cellular automata was analysed in a two-dimensional case in Ref. [14]. The approach was used to simplify the calculations; the extension to three dimensions is reasonably straightforward. Given a block model of certain dimensions, the probability of a given bubble to reach the position of block (i, j) is given by:

$$Pr\{\eta(i,j)=1\}=\sum_{k=i-1}^{i+1} Pr\{\eta(i,j)=1/\eta(i,j-1)=1\}\cdot Pr\{\eta(i,j-1)=1\} \tag{12}$$

where $\eta(i, j)$ is an indicator function defined as:

$$\eta(i,j)=\begin{cases}1, \text{ if pass through}\\ 0, \text{ if not}\end{cases} \tag{13}$$

This calculation becomes trivial using Total Probabilities Rule. The quantity $Pr\{\eta(i, j)=1\}$ is called bubble probability. Considering p_1, p_2, p_3 as transition probabilities for the neighbours (left, centre, right), then,

$$\begin{aligned}Pr\{\eta(i,j)=1\} &= p_1 Pr\{\eta(i,j-1)=1\}+\\ &+p_2 Pr\{\eta(i-1,j-1)=1\}+\\ &p_3 Pr\{\eta(i+1,j-1)=1\}\end{aligned} \tag{14}$$

To understand the kind of phenomenon this model simulation is very important to characterize the final cavity generated by the extraction of material. Empirical tests provide cavities with parabolic form but formal definitions are required to explain this behaviour. To illustrate the importance of this point, a two-dimensional case with transition probabilities given by p_1=0.8, p_2=p_3=0.1 was considered (Fig. 6). The blocks that obtain a positive probability of being visited by a bubble are those depicted in Fig. 7 (a). For the blocks that have bubble probability greater than 0.001, the shape is described by Fig. 7 (b). Finally cases in Figs. 7(c) and (d) are for bubble probabilities greater than 0.05 and 0.07, respectively.

ALFARO and SAAVEDRA [14] observed that the differences between the shapes for different cut-off bubble probabilities required a more formal approach. They proposed the concept of the significance level that

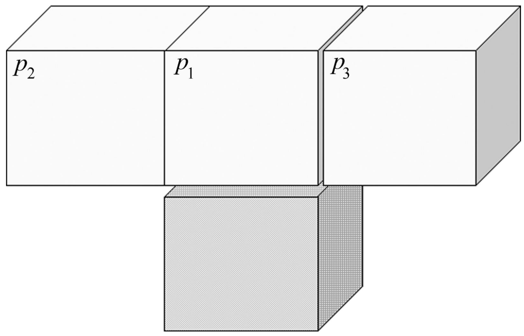

Fig. 6 Block neighbourhood in two dimensional case [14]

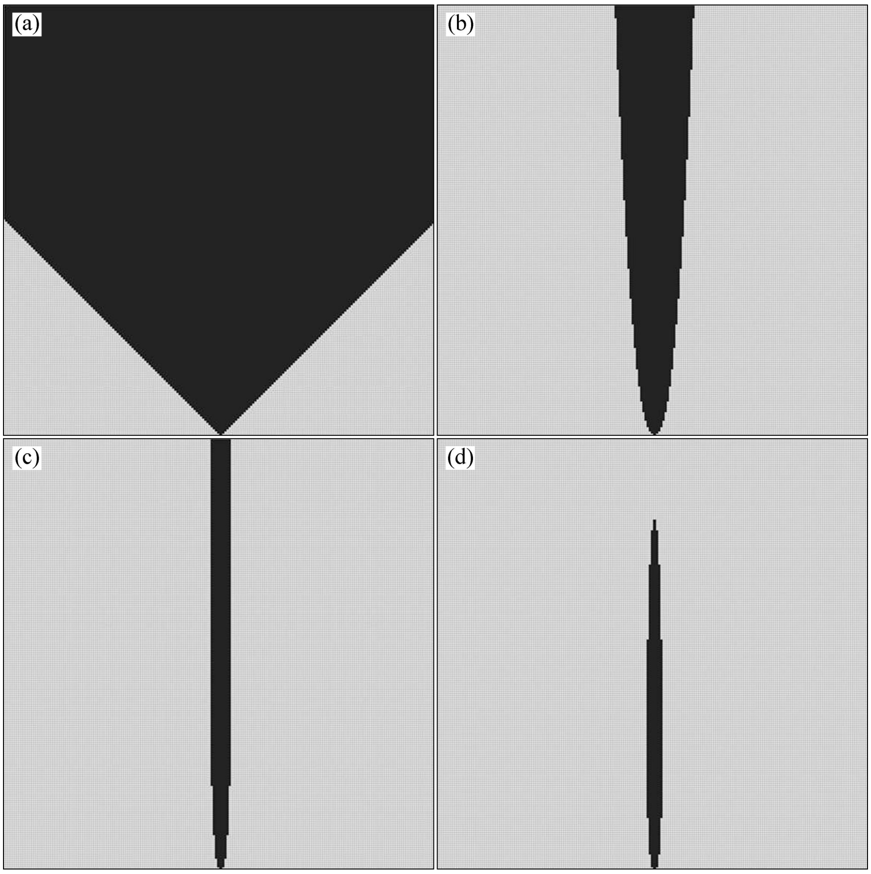

Fig. 7 Final cavities considering distinct bubble probabilities [14]: (a) $Pr\{\eta(i, j)=1\}>0$; (b) $Pr\{\eta(i, j)=1\}>0.001$; (c) $Pr\{\eta(i, j)=1\}>0.05$; (d) $Pr\{\eta(i, j)=1\}>0.07$

will be shortly explained. Equation (13) gives a probability distribution that in each level approximates a Gaussian one, i.e., the central block (the one in the same column as the draw point) has a greater probability of being visited by a particular bubble, and this probability decreases as it moves away from the central column.

The model can be seen as a random walk in one dimension (in the two dimensional case) and a random walk in two dimensions (in the three dimensional case). The way to understand this fundamental fact is to see that if all levels are put together into one level then the system evolves in the same way a random walk process would happen. Such kind of processes are described by means of a partial differential equation (PDE) for the probability density function of the position of the bubble, $p(x, t)$, in time t when starting from initial position x:

$$\frac{\partial}{\partial t} p(x,t) = v\frac{\partial}{\partial x} p(x,t) + D\frac{\partial^2}{\partial x^2} p(x,t) \tag{15}$$

With solution:

$$p(x,t) = \frac{1}{\sqrt{4\pi Dt}} \exp\left(-\frac{(x-vt)^2}{4Dt}\right) \tag{16}$$

The border condition for Equation (16) is $p(x,0)=\delta(x)$.

It can be seen that this solution manifests the clear link between the CA model and the subsidence phenomenon as presented by KNOTHE [1]. In fact, the CA model by representing the extraction process implicitly can model the surface subsidence as a by-product. This unexpected connection opens a new realm of the application of new, flexible, computationally advantageous technology to this old problem that could reinvigorate this research area.

6 Conclusions

1) The application of the proposed dynamic subsidence prediction model, that is extended from the model originally proposed by KNOTHE [1] and considers the sub-critical cases, provides further improvement with subsidence prediction accuracy. The model rendered results characterised by a maximum deviation of 12%. However, the authors believe that the model can be further improved by considering the rock strata composition. Such consideration should correct the larger deviations observed at the edges of the extraction

panel.

2) It can be seen that the theoretical solution obtainable using the reviewed CA model shares a common form with model based on the Gauss influence function (adopted by KNOTHE). This encourages future research, as it will allow for the introduction of fine granularity in the study of subsidence phenomenon. It is expected that the models based on CA will allow for more flexibility and be able to take into account the geological and geotechnical conditions of the overburden strata.

3) The cellular automaton reviewed in this paper is based on the probabilistic evolution rules. Two different computational runs of the CA based simulations will provide two different results. Several runs will provide a set of scenarios that can be used to estimate and characterise the precision associated with subsidence prediction. Such information could be used to take decisions that incorporate risk measurements, thus providing a new set of tools to assess extraction plans in terms of subsidence to mention just one example.

References:

[1] KNOTHE S. Effect of time on formation of basin subsidence [J]. Archives of Mining and Steel Industry, 1953, 1(1): 1−7. (in Polish)

[2] JAROSZ A, KARMIS M, SPROKA A. Subsidence development with time-experiences from longwall operations in the Appalachian coalfield [J]. International Journal of Mining and Geological Engineering, 1990(8): 261−723.

[3] CHANG Zhan-qiang, WANG Jin-zhuang. Study on time function of surface subsidence — The Improved Knothe time function [J]. Chinese Journal of Rock Mechanics and Engineering, 2003, 22: 1496−1499. (in Chinese)

[4] CUI X, WANG J, LIU Y. Prediction of progressive surface subsidence above longwall coal mining using a time function [J]. International Journal of Rock Mechanics & Mining Sciences, 2001(38): 1057−1063.

[5] DJAMALUDDIN I, MITANI Y, ESAKI T. Evaluation of ground movement and damage to structures from Chinese coal mining using a new GIS coupling model [J]. International Journal of Rock Mechanics & Mining Sciences, 2011, 25(2): 25−36.

[6] YU Xue-yi, DANG Tian-hu, PAN Hong-yu, et al. Theological characteristics of surface dynamic subsidence by mining [J]. Journal of Xi'an University of Science & Technology, 2003(2): 131−134. (in Chinese)

[7] ZENG Z, KOU X. Application of viscoelasticity to study the time-dependent surface subsidence caused by underground mining [J]. Engineering Geology, 1992(32): 279−284.

[8] DENG Ke-zhong, WANG Jin-zhuang, XING An-shi. On predicting the surface subsidence velocity in undermining process [J]. Journal of China University of Mining & Technology, 1983(4): 68−79. (in Chinese)

[9] ADAMEK V, JERAN P W, TREVITIS M A. Development of dynamic subsidence over longwall panels in the northern Appalachia Coal Region [J]. Rock Mechanics, 1992: 243−251.

[10] FALON S, GAVETE L, RUIZ A. A model to simulate the mining subsidence problem: coding and implementation of the algorithm [J]. Computers & Geosciences, 1996, 22(8): 897−906.

[11] YANG G, CHUGH Y P, YU Z, et al. A Numerical approach to subsidence prediction and stress analysis in coal mining using a laminated model [J]. Int J Rock Mech Mitt Sci & Geomech Abstr, 1993, 30(7): 1419−1422.

[12] LI Jian-you, YAN Jia-ping, XIE Yan, et al. Dynamic action simulation system and preliminary experiments of coal seams and gas [J]. Mining Science and Technology, 2009, 19(2): 473−478.

[13] DAI Hua-yang, Wamg Jin-zhuang. Prediction model for surface movement and deformation induced by sub-critical extraction [J]. Journal of China Coal Society, 2003(6): 583−587. (in Chinese)

[14] ALFARO M, SAAVEDRA J. Predictive models for gravitational flow [C]//MassMin 2004. Santiago, Chile, 2004.

[15] BAXTER G, BEHRINGER R. Cellular automata models of granular flow [J]. Physical Review A, 1990: 1017−1020.

[16] LAMARCHE K, CONWAY S, GLASSER B, SHINBROT B. Cellular automata model of gravity-driven granular flows [J]. Granular Matter, 2007: 219−229.

[17] GOLES E, GONZALEZ G, HERRMANN G, MARTINEZ S. Simple lattice model with inertia for sand piles [J]. Granular Matter, 1998: 137−140.

[18] KOZICKI J, TEJCHMAN J. Application of a cellular automaton to simulations of granular flow in silos [J]. Granular Matter, 2005: 45−54.

[19] GOLES E, PEÑA S. Modeling and simulation of gravitational flow (Spanish) [D]. Santiago, Chile: Final Report PB5-10004, Apendix 2, 1996.

[20] GONZALEZ G. Study of the behavior of a granular material through computational models (Spanish) [D]. Santiago, Chile: Thesis to Obtain the Degree of Mathematical Civil Engineer, 1999.

[21] SAAVEDRA J. Sequences, gravitational flow and evolution in mine planning (Spanish) [D]. Santiago, Chile: Thesis to Obtain the Degree of Mathematical Civil Engineer, 2002.

[22] SAAVEDRA J, ALFARO M, AMAYA J. An evolutionary model for underground mining planning [C]//MassMin 2004. Santiago, Chile, 2004.

[23] WOLFRAM S. A new kind of science [C]//Wolfram Media, Inc., 2002.

[24] CALDERON C, ALFARO M, SAAVEDRA J. Computational model for simulation and visualization of gravitational flow [C]//MassMin 2004. Santiago, Chile, 2004.

(Edited by LONG Huai-zhong)